Supporting Information

Chung et al. 10.1073/pnas.1002347107

SI Text

Materials. Sulfopropyl Sepharose Fast Flow (SP Sepharose FF), Capto MMC (multimodal cation exchanger), and Sephadex G-50 Superfine media were obtained from GE Healthcare. The SP Sepharose FF and Capto MMC media were packed into separate Pharmacia Biotech glass columns (5 mm × 50 mm). The Sephadex G-50 Superfine media was packed into a BioRad glass chromatography column (1.5 cm × 75 cm). A SP Sepharose FF HiLoad 16/10 column was obtained from Pharmacia (GE Healthcare). Stable isotopically labeled ammonium chloride and glucose were purchased from Isotec (Sigma-Aldrich). Iron (III) chloride, ammonium chloride, potassium phosphate, potassium sulfate, calcium chloride, tris(hydroxymethyl)aminomethane, hydrochloric acid, protease cocktail inhibitor, deoxyribonuclease (DNAse), sodium chloride, sodium azide, acetic acid, sodium acetate, deuterium oxide (D_2O), 3-(trimethylsilyl)propionic acid-d_4 sodium salt (TMSP), NMR tubes, N-benzoyl DL methionine, and 1-propanesulfonic acid were purchased from Sigma-Aldrich. Magnesium chloride (hexahydrate) was purchased from Mallinckrodt Baker. IPTG was obtained from BioWorld. Native human ubiquitin and mutants were purchased from Boston Biochem. MOPS, tricine, dextrose, thiamine hydrochloride, ampicillin, sodium hydroxide, and sterile Nalgene filter packs were purchased from Thermo Fisher Scientific. Centriprep centrifugal filter devices were purchased from Millipore.

Equipment. Analytical linear gradient experiments were performed using a Waters High Performance Liquid Chromatography system consisting of a 600 multisolvent delivery system, a 717 Waters Intelligent Sample Processor autoinjector, and a 996 photodiode array detector controlled by a Millennium chromatography software manager. NMR spectra were obtained using a Bruker 800-MHz spectrometer equipped with a HCN cryoprobe and z-axis gradients. NMR data acquisition and analysis was carried out with the Bruker Topspin 2.1 software package.

Coarse-Grained Docking Simulations. Coarse-grained docking simulations were performed using the Autodock package developed by Morris and co-workers (1, 2). To find a suitable binding conformation, a genetic search algorithm was applied to reduce the free energy of a randomized ligand starting position. At each step of the search algorithm, an empirical function, based on the weighted summation of different energy functions, was used to predict the free energy of an adopted protein-ligand confirmation. The energy functions used here included van der Waals, hydrogen bonding, electrostatics, desolvation, and torsional free energies. Each of these properties was given empirical weightings in the total energy calculation, determined from a fitting of known ligand-protein interactions. While this and other docking applications are typically used for high energy binding at a known binding site, the versatility of the genetic search algorithm makes it ideal for use in blind-docking simulations where there may be several low energy binding sites at unknown locations on the protein's surface.

For the current study the protein was protonated according to the experimental pH and then energy minimized using AMBER 99 force field parameters (3). The ligands were modeled as truncated forms of the resin ligands and are shown in Fig. 1 *A* and *B*. For the analysis of local docking sites the simulation space was limited to an area covering the experimentally determined binding sites from NMR and the neighboring residues. In order to maximize the correlation between the docked and experimental confirmations, flexible residues were applied to the binding site residues on the protein surface. Each docking simulation was performed with a large number of energy calculations (approximately 27,000 generations in the genetic algorithm) in order to assure that the confirmations determined were at a minimum energy for both the ligand and amino acid side chains. Each of these docking simulations were carried out 20 times for each binding site examined. The results of these simulations were then analyzed for visualization, energetics, and cluster analysis using the AutodockTools package of the Python Molecular Viewer program (4, 5).

1. Huey R, Morris GM, Olson AJ, Goodsell DS (2007) A semiempirical free energy force field with charge-based desolvation. *J Comput Chem* 28:1145–1152.
2. Morris GM, et al. (1998) Automated docking using a Lamarckian genetic algorithm and an empirical binding free energy function. *J Comput Chem* 19:1639–1662.
3. Cornell WD, et al. (1995) A 2nd generation force-field for the simulation of proteins, nucleic-acids, and organic-molecules. *J Am Chem Soc* 117:5179–5197.
4. Sanner MF (1999) Python: A programming language for software integration and development. *J Mol Graph Model* 17:57–61.
5. Sanner MF, Olson AJ, Spehner JC (1996) Reduced surface: An efficient way to compute molecular surfaces. *Biopolymers* 38:305–320.

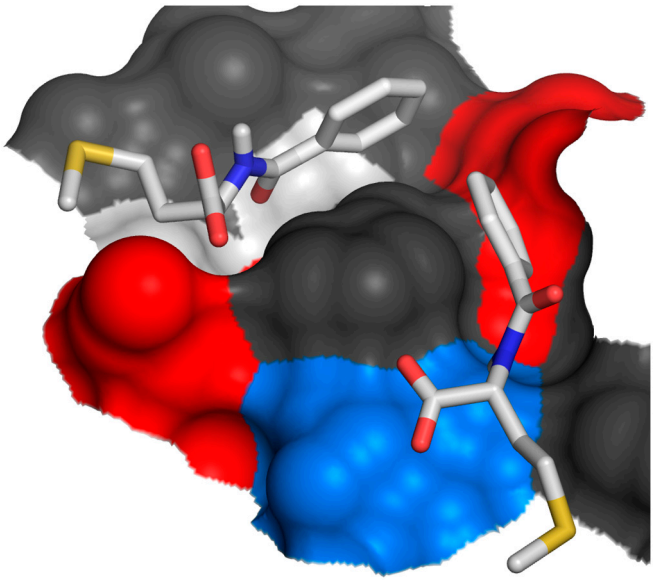

Fig. S1. Coarse-grained docking results showing multiple multimodal chromatographic ligands binding to His 68, a residue that shows multiphasic behavior for ligand-induced changes in chemical shift by NMR. Surface colors correspond to NMR results (Fig. 5).

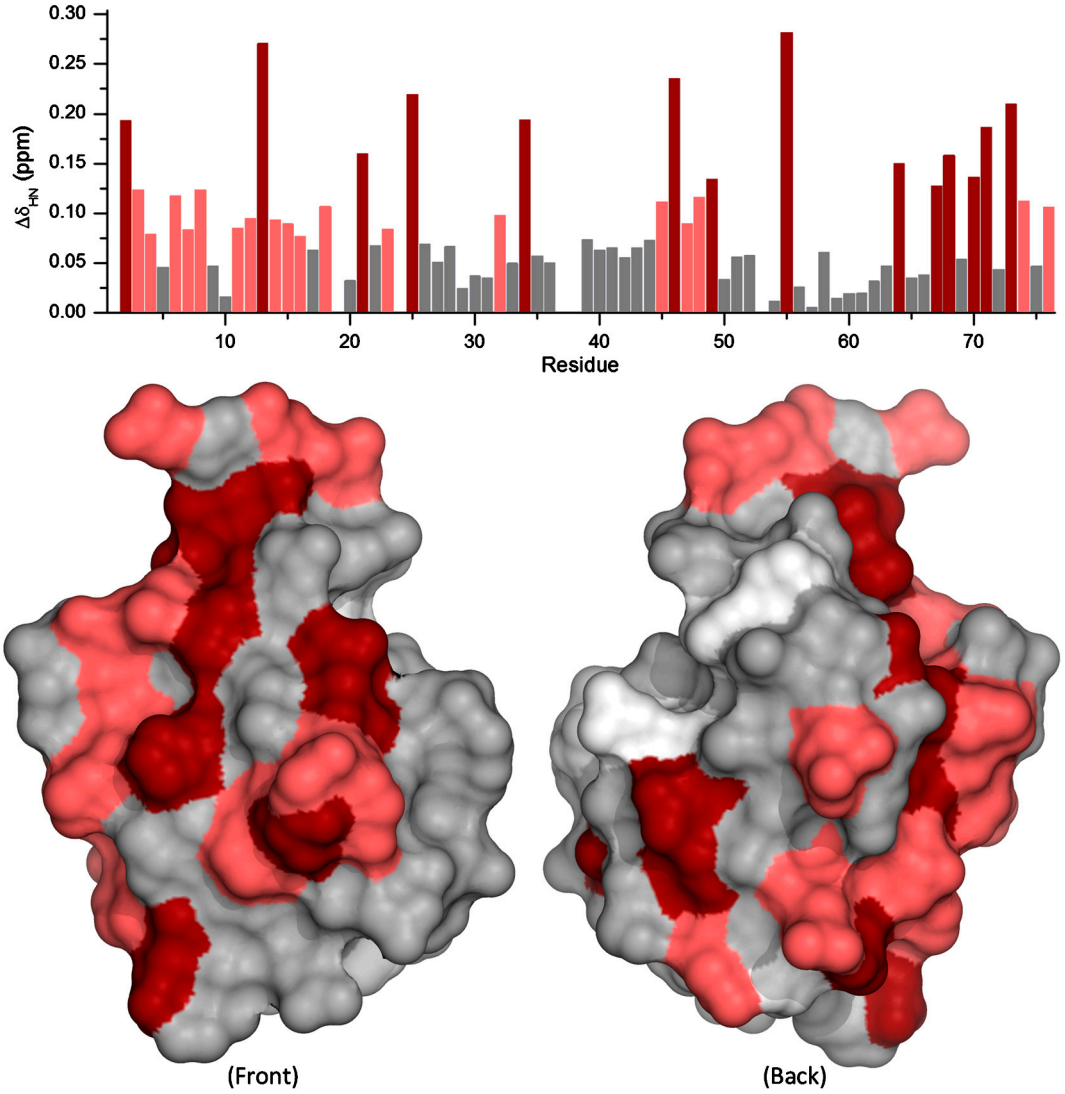

Fig. S2. A summary graph and colored surface representation of the residue specific ligand-induced changes in amide chemical shift are presented for the binding of the Capto MMC ligand with the relative magnitudes calculated as a normalized sum of the ^{1}H and ^{15}N. Data differentiated by low (gray), medium (pink), and high (red) responses. The combined chemical shift was calculated using: $\Delta\delta_{HN} = \sqrt{(\Delta\delta_H)^2 + (0.2 \cdot \Delta\delta_N)^2}$.

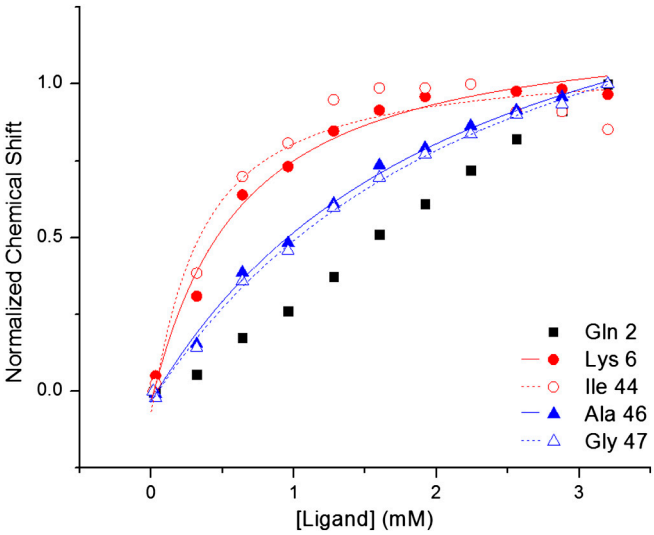

Fig. S3. Representative ligand-induced changes in chemical shift data and fits for several residues within binding sites 1 (red) and 2 (blue) compared to a noninteracting residue (black). Lines represent resulting fits using a single-site binding model as described in *Materials and Methods*.